Vol. 40, No. 2 (2018) 239-246, DOI: 10.24874/ti.2018.40.02.07

Tribology in Industry

www.tribology.rs

RESEARCH

Erosion-corrosion Behaviour of Dual Phase Medium Carbon Steel using a Designed Slurry Pot

S. Aribo[a,b], I. Adedapo[a], C. Nwogwugwu[a], O. Olaniran[a], A. Olaseinde[a], O. Ige[b], P.A. Olubambi[b]

[a] *Department of Metallurgical and Materials Engineering, Federal University of Technology, Akure, Nigeria,*
[b] *Centre for Nanoengineering and Tribocorosion, School of Mining, Metallurgy and Chemical Engineering, University of Johannesburg, Johannesburg, South Africa.*

Keywords:

Slurry pot
Dual phase steel
Erosion-corrosion
Medium carbon steel
Inter-critical temperature
Hardness

Corresponding author:

Sunday Aribo
Centre for Nanoengineering and Tribocorosion, School of Mining, Metallurgy and Chemical Engineering, University of Johannesburg, South Africa.
E-mail: aribosunny@yahoo.com

A B S T R A C T

A slurry pot has been designed, fabricated and evaluated for erosion-corrosion investigations. A variable voltage controller was used to vary the input voltage into the one-horse-power motor that controls the slurry pot. The actual speed of the slurry pot shaft was also calibrated using a non-contact digital tachometer. Voltages of 100 and 200 V resulted in rotational speeds of 1100 and 2100 rpm, respectively employed for the subsequent erosion-corrosion tests. Erosion-corrosion of a dual-phase carbon steel was investigated with the aid of the slurry pot in aerated 3.5 wt.% NaCl environments. The sample was normalised at 850 °C and then cooled in air to room temperature. Prior to the test, the normalised samples were heated to 700, 725, 750, 775, 800 and 825 °C, respectively and quenched in oil. Erosion-corrosion rates of between 0.027 to 1.26 g/cm².hr at 1100 rpm and 0.57 to 1.9 g/cm².hr at 2100 rpm were recorded. It was also observed that as hardness increased there was reduction in weight loss of the heat treated alloy.

1. INTRODUCTION

Erosion-corrosion is a complex material degradation mechanism arising from both chemical and mechanical interactions [1,2]. Mining, hydropower and oilfield environments are among the areas where this material degradation mechanism is prevalent [3-5]. Slurry erosion pot is one of the numerous methods that can be deployed to study erosion-corrosion. The slurry pot has an advantage of a simple arrangement for potentiometric control of the specimens as well as ability to attain higher rotational speed. This experimental rig is also recommended for the understanding of the mechanism of erosion-corrosion interaction for dilute slurries [6,7]. Meanwhile, recent investigations show that most researchers investigating erosion-corrosion effects in laboratory design and fabricate customized slurry pot erosion-corrosion rig as this is not yet captured in ASTM standard [8].

Medium carbon steels are hardenable and they can be partially hardened by quenching within the intercritical temperatures (AC_1 and AC_3) of the Fe–C equilibrium diagram. Within this processing window, ferrite, martensite, retained

austenite, bainite and pearlite are present [9-12] and such multiple phases make such alloy to exhibit unique properties. This is because ferrite is ductile and martensite is a hard phase [10-12]. Dual phase steel has high hardness because of the presence of martensite island within the ferrite matrix [9]. The presence of retained austenite in such matrix also makes such alloy strain hardenable because austenite is a metastable phase [13-16]. Several attempts have been made in the past to relate the volume fraction of martensite in such alloy to its tribological behaviour [9,17,18]. It has been reported that the wear resistance of dual phase steel increases as the volume fraction of martensite increases [17,18] albeit at low load.

However, little information is available to correlate the microstructural properties of dual phase carbon steel with their slurry erosion properties [9]. There are also different opinions as to how the hardness of steels affects their erosion-corrosion characteristics. Some schools of thought [19,20] believed that hardness affect the erosion-corrosion resistance of the alloy while some researchers [21-23] reported that this factor is not significant although it does affect it. High hardness has also been reported to result in low erosion rate for ductile metals [24]. This research is an attempt to produce a slurry pot for erosion-corrosion research as well as to expand the data base on the erosion-corrosion characteristics of multiphase carbon steel.

2. MATERIALS AND METHODS

2.1 The slurry pot test rig

Outer shell of the pot is made of mild steel while the inner part is made of plastic to reduce corrosion of the inner wall. Inner diameter of the pot has a depth of 35 cm and diameter of 29 cm as selected from the plastic container, Figs. 1 and 2. Total capacity of the slurry pot in terms volume is thus approximately 23 litres.

The sample holder as shown in Fig. 3 was made of perspex with a centre hole of diameter 20 mm to fit the shaft attached to the electric motor. A plastic screw was also used to support the shaft for more rigidity. The sample holder has four radial arms equidistance from the centre. Two of which are circular in shape while the other two are rectangular in shape as shown in Fig. 3a. This is to allow the use of both rectangular and circular specimens.

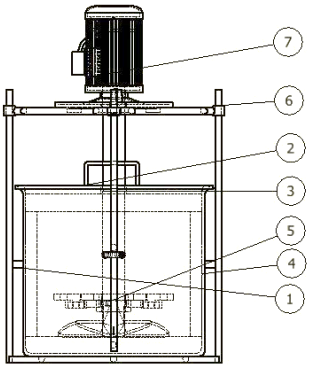

PARTS LIST			
ITEM	QTY	PART NAME	DESCRIPTION
1	1	pot	
2	1	pot lid	
3	1	shaft and blade	
4	1	inner casing	
5	1	sample holder	
6	1	motor rest	
7	1	motor	1 HP (1 hourse power)

Fig. 1. Designed and fabricated slurry pot (2D).

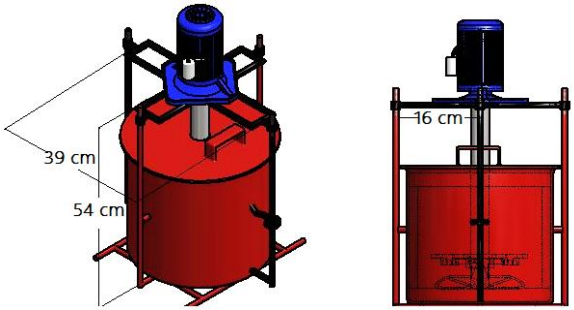

Fig. 2. Designed and fabricated slurry pot (3D).

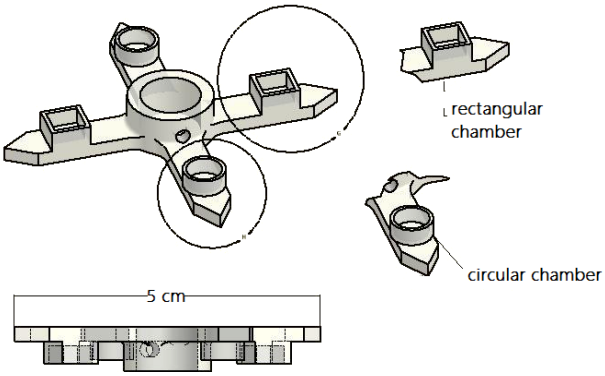

a) Sample holder for the slurry pot

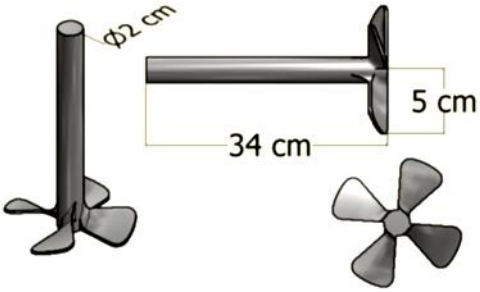

b) Shaft for the holder

Fig. 3. Designed sample holders for the slurry pot

The shaft in Fig. 3b was made from a hollow zinc plated steel pipe force-fitted into a plastic casing. The shaft is of length 34 cm and diameter of 20

mm. A stirrer made of plastic material is fixed to the lower end of the shaft while the upper end is connected to the electric motor.

2.2 Assembled slurry pot and its mode of operation

The specimen to be tested is prepared by grinding and cleaning appropriately and weighed using a precision weighing machine. Sample having the standard size is then fixed onto the sample holder and immersed in the slurry. The motor is switched on and samples are rotated with the aid of a propelling shaft at the desired speed for a given period of time. After each experiment, the specimen is removed, cleaned and weighed. The rate of erosion-corrosion is thus calculated.

2.3 Speed control and calibration of the slurry pot

A voltage regulator (variac) is connected to the motor to step the voltage between 0-240 V. A non-contact tachometer is used to calibrate the input speed. This is done by pointing the ray of the tachometer on the rotating shaft and the speed is read off from the digital display of the tachometer. Three readings are taken at a particular voltage and the average is then calculated. At voltages 100 and 200 Volts speeds of approximately 1100 and 2100 rpm, respectively were recorded. These were used for the erosion-corrosion experiments.

2.4 Heat treatment operations

Medium carbon steel with chemical composition (analyzed with Auger spectrometer) shown in Table 1 was tested using the designed slurry pot. The medium carbon steel samples were sectioned into 10 x 20 mm. Samples were normalized by heating the specimens to austenitizing temperature of 850 ^{o}C, soaked for 30 minutes and then cooled in air to room temperature. A set of the normalized samples was heated to 700 ^{o}C, soaked for 30 min and then quenched in oil. This same procedure was carried out for other sets of samples at 725, 750, 775, 800 and 825 ^{o}C, respectively. Meanwhile the lower critical temperature (AC_1, 720 ^{o}C) and the upper critical temperature (AC_3, 782 ^{o}C) were determined using the empirical formulae in equations 1 and 2 [25].

$$AC_1\ (^{o}C) = 739 - 22\ C - 7\ Mn + 2\ Si + 14\ Cr + 13\ Mo - 13\ Ni + 20V \quad (1)$$

$$AC_3\ (^{o}C) = 902 - 255C - 11Mn + 19\ Si - 5Cr + 13\ Mo - 20\ Ni + 55V \quad (2)$$

Table 1. Chemical composition (weight %) of medium carbon steel.

C	Si	Mn	S	P	Cr	Ni	Cu
0.397	0.28	0.867	0.055	0.034	0.143	0.098	0.297
Nb	**Al**	**B**	**W**	**Mo**	**V**	**Ti**	**Fe**
0.0001	0.010	0.0001	0.0001	0.0001	0.0001	0.007	97.31

2.5 Metallographic examination

Samples were mounted in phenolic resin and ground on a water lubricated hand grinding set-up of abrasive papers. Grinding papers with grit sizes 240, 600, 800 and 1200 grades were used in that order. Polishing was carried out on a rotating disc of a synthetic velvet polishing cloth impregnated with alumina paste. Final polishing was carried out with diamond paste of 15 µm. The specimens were then etched with Nital. Microstructural analyses were performed with Tescan Electron Microscope, Oxford Instrument available at the University of Johannesburg.

2.6 Hardness test

Samples were ground and polished as described in section 2.5 and the hardness test performed using Rockwell hardness tester. The samples were loaded into the hardness tester and a load of 150 gf was used. The sample was then punched and the readings were recorded and the procedure was repeated three times to validate the results.

2.7 Erosion-corrosion tests

Erosion-corrosion tests were carried out using the designed slurry pot in Figs. 1-3. The slurry pot was operated at average speeds of 1100 and 2100 rpm. The test solution contains 3.5 wt.% NaCl and 500 mg/l silica sand with particle distribution as reported by Aribo et al. [26]. Prior to immersion the test samples was ground to a surface finish of 1200 grit using silicon carbide paper, polished with 15 µm diamond paste, degreased, washed in distilled water and dried in air. Each experiment was performed for 1 hour and the weight loss measured before and

after the experiment. The erosion-corrosion rate was calculated using the formula:

$$\text{Erosion-corrosion rate} = \frac{\text{Weight loss (g)}}{\text{Surface area (cm}^2\text{) x time (hr.)}} \quad (3)$$

3. RESULTS AND DISCUSSION

3.1 Calibration of the slurry pot

Results obtained from the calibration of the motor is shown in Fig. 4.

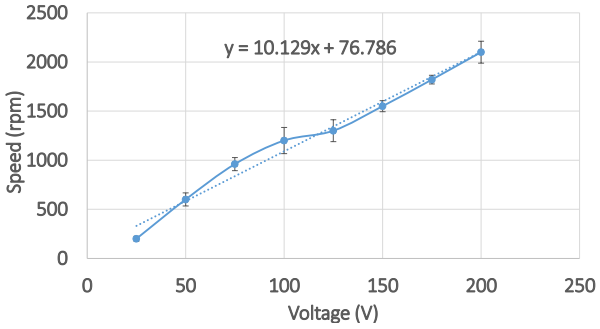

Fig. 4. Calibration plot for the motor.

As shown in Fig. 4, a graph of rotation speed (rpm) against the applied voltage revealed that speed up to 2500 rpm is achievable at a voltage of 240 V. This is a relatively high velocity which is characteristic of a slurry pot erosion rig. For this research, speeds of 1100 and 2100 rpm were used.

3.2 Hardness properties

The results of the hardness test performed on the medium carbon steel samples using the Rockwell hardness tester helped to establish the effect of the heat treatment on the medium carbon steel sample.

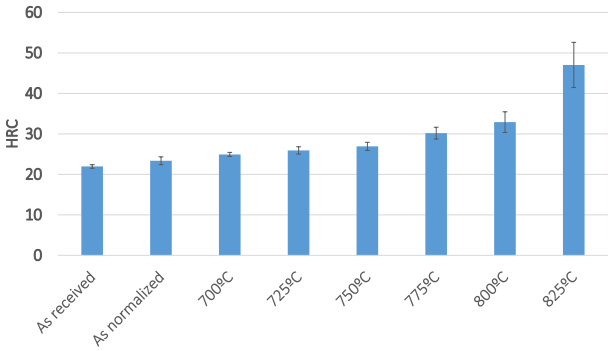

Fig. 5. Hardness values (HRC) for the medium carbon steel.

It is shown from the result in Fig. 5 that as the heat treatment temperature increased through the dual phase (α+Υ) region to the austenitic (Υ) region, the hardness of the steel sample increases. It is expected that higher austenite volume fraction and lower ferrite volume fraction will be achieved with higher temperature. Higher volume fraction of austenite is expected to transform to higher martensite volume fraction during quenching. Hence, higher hardness as expected of a martensitic phase.

3.3 Erosion-corrosion properties

Results of the erosion-corrosion tests performed on the medium carbon steel samples are shown in Figs. 6 and 7. Good repeatability is seen in all the experiments conducted as shown by the deviations from the mean values shown by the error bars in Figs. 5 and 6. Also, higher slurry speed of 2100 rpm resulted in higher erosion-corrosion rates than the lower speed of 1100 rpm as expected. It can therefore be said that the slurry pot fabricated functioned as it is designed for.

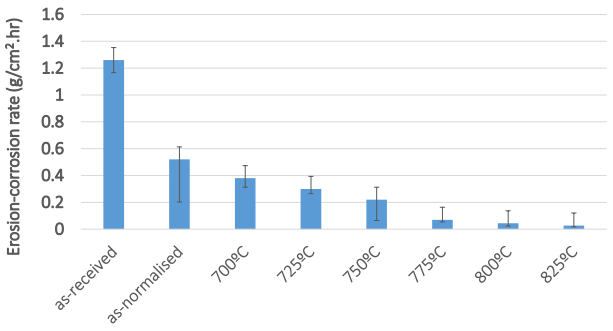

Fig. 6. Effects of heat treatment on the erosion-corrosion characteristics of the heat treated medium carbon steel at 1100 rpm.

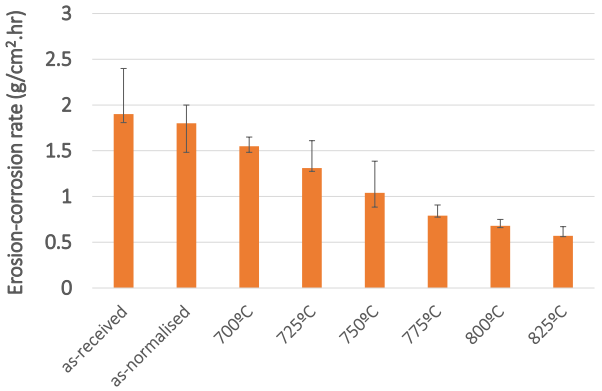

Fig. 7. Effects of heat treatment on the erosion-corrosion characteristics of the heat treated medium carbon steel at 2100 rpm.

Figures 6 and 7 also showed that increase in hardness of the steel resulted in higher

resistance to erosion-corrosion. It will be recalled that higher hardness was recorded when the heat treatment temperature increases from the dual phase region towards the austenite region which would imply higher volume fraction of martensite after quenching.

3.4 SEM images of the samples as normalised and hardened

The microstructure of the normalised sample and alloy austenitized and quenched are shown in Fig. 8. Normalised sample shown in plate A consists of mainly pearlitic phase. So also is the alloy heated to 700 °C and quenched in oil (plate B). Both samples were expected to feature such phase as alloy heated to 700 °C is below the AC_1 line and hence, no transformation would occur. Plate C is the micrograph of the alloy heated to 750 °C and then quenched in oil. This alloy is heated within the α+Ɣ region and the micrograph showed ferrite, retained austenite and very little volume fraction of lathe of martensite as expected.

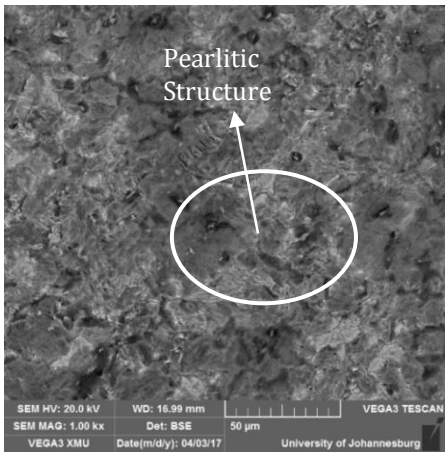

a) SEM (BSE) images of the alloys as Normalized.

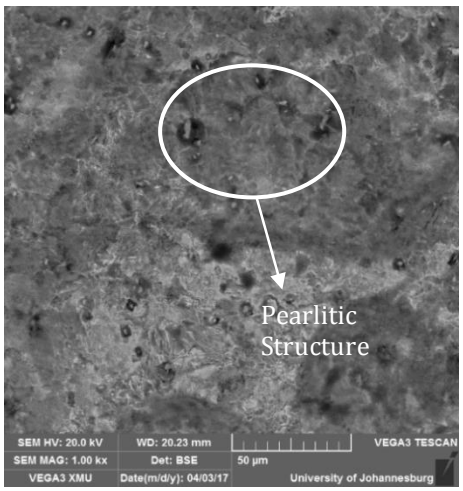

b) SEM (BSE) images of the alloys heated to 700 °C and quenched.

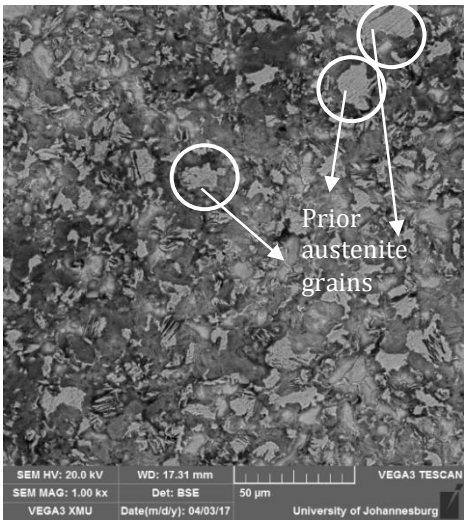

c) SEM (BSE) images of the alloys heated to 750 °C and quenched.

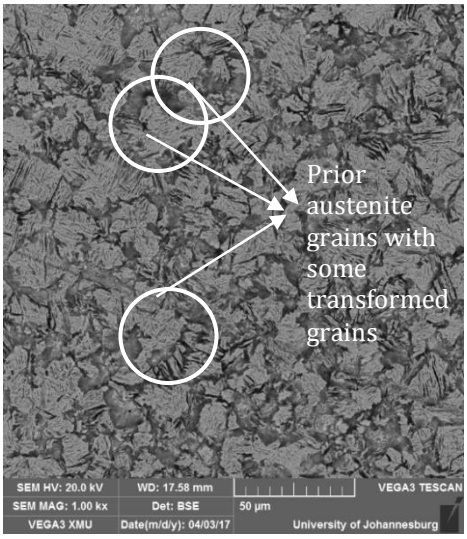

d) SEM (BSE) images of the alloys heated to 800 °C and quenched.

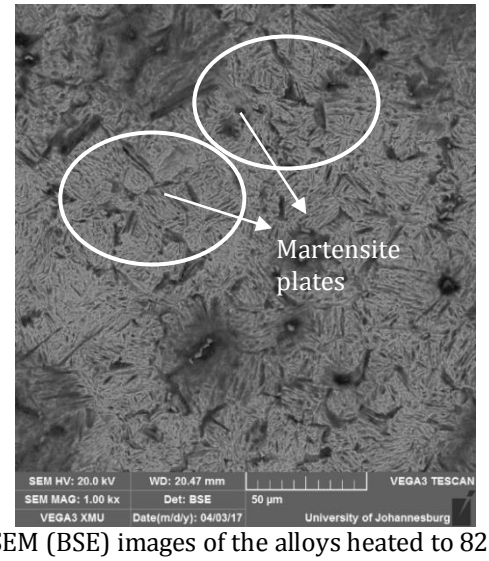

e) SEM (BSE) images of the alloys heated to 825 °C and quenched

Fig. 8. SEM (BSE) images of the alloys.

During austenitization, ferrite and austenite phases are expected to form and when such phases are quenched, the austenite transformed to martensite retaining the ferrite phase. The same features are repeated in plate D (with higher volume fraction of martensite) for the alloy heated to 800 °C and then quenched in oil. For both plates C and D the prior austenite grains can still be seen (with the plates of martensite aligned within the grains). After the quenching, it was also noticed that the higher volume fraction of austenite grains are retained within the matrix of the alloy quenched at 800 °C compared with alloys quenched at 750 °C. Plate E (825 °C) shows a full martensitic structure as expected of the alloy austenitized within the austenite region. Needle-like structure of martensite was observed in more than 95 % of the phase.

3.5 Relationship between the microstructure and erosion-corrosion resistance

There seems to be a direct effect of the higher martensite volume fraction and invariably higher hardness on the erosion-corrosion rate in both environments. It is also noticed that at lower temperature where the volume fraction of ferrite and pearlite is expected to be higher, erosion-corrosion resistance was low. This was because ferrite has been reported to be soft and strain rate sensitive and hence susceptible to erosion [14-16]. The rate of austenite transformation to martensite plays a significant role in determining the erosion-corrosion performance of the heat treated samples. This is in line with previous publication that reported the effects of phase's volume fractions in assessing the mechanical properties [27]. The results as obtained in this study tend to be more supportive of the work of Tekeli and Gural [28] in that martensite hardness has relatively greater influence on the erosion-corrosion rate.

3.6 Degradation mechanism

Degradation mechanism shows both scratching and ploughing (Fig. 9a) as well as pits (Fig. 9b). Scratches and ploughing from the sand is expected at the high rotational speed and high volume fraction of sand particles. This is a classical mode of degradation in a slurry erosion. There is also the effect of the corrosive medium on the heat treated medium carbon steel with general and localised corrosion seen on the steel surface.

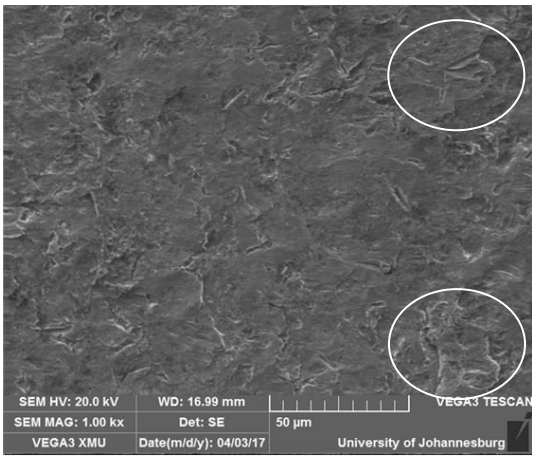

a) scratching and ploughing

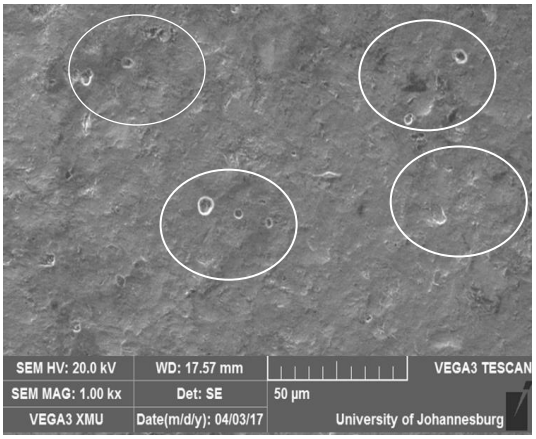

b) pits

Fig. 9. SEM (SE) images of medium carbon steel subjected to slurry erosion-corrosion at 2100 rpm.

It can therefore be said that there is a form of synergy between erosion and corrosion although the extent has not been quantified in this study.

4. CONCLUSIONS

A slurry pot has been successfully designed, fabricated, calibrated and evaluated for erosion and erosion-corrosion tests in the laboratory. Medium carbon steel from different heat treatment conditions and resultant microstructures possess different hardness values and were tested using the developed rig. It was observed from the results that higher hardness resulted in lower degradation while higher slurry speed resulted in higher material loss due to erosion-corrosion. Degradation of the alloy combines both erosion and corrosion with ploughing and pitting dominating the degradation mechanism.

REFERENCES

[1] M.M. Stack, N. Pungwiwat, *Erosion–corrosion mapping of Fe in aqueous slurries: some views on a new rationale for defining the erosion–corrosion interaction,* Wear, vol. 256, iss. 5, pp. 565–576, 2004, doi: 10.1016/S0043-1648(03)00566-0

[2] E. Mahdi, A. Rauf, S. Ghani, A. El-naomany, A. Pakari, *Erosion-corrosion Behavior and Failure Analysis of Offshore Steel Tubular Joint*, International Journal of Electrochemical science, vol. 8, pp. 7187-7210, 2013.

[3] S. Aribo, M. Bryant**,** X. Hu, A. Neville, *Erosion-corrosion behaviour of lean duplex stainless steel (UNS S32101) in a CO_2-saturated oilfield environment,* in NACE International Conference, March 17-21, 2013, Orlando Florida, USA, Paper no. 2382.

[4] X.G. Guo, B.T. Guo, L.J. Luo, *Interaction of mechanical and electrochemical factors in erosion–corrosion of carbon steel*, Electrochim Acta, vol. 51, iss. 2, pp. 315-323, 2005, doi: 10.1016/j.electacta.2005.04.032

[5] M.M. Stack, J.S. James, Q. Lu, *Erosion–corrosion chromium steel in a rotating cylinder electrode system: some comments on particle size effects,* Wear vol. 256, iss. 5, pp. 256-557, 2004, doi: 10.1016/S0043-1648(03)00565-9

[6] H.McI. Clark, *Particle velocity and size effects in laboratory slurry erosion measurements OR… do you know what your particles are doing?* Tribology International, vol. 35, iss. 10, pp. 617–624, 2002, doi: 10.1016/S0301-679X(02)00052-X

[7] N. Ojala, K. Valtonen, P. Kivikytö-Reponen, P. Vuorinen, V.-T. Kuokkala, *High speed slurry-pot erosion wear testing with large abrasive particles*, Tribologia, vol. 33, iss. 1, pp. 36-44, 2015.

[8] M.H. Buszko, A.K. Krella, *Slurry erosion-design of test devices*, Advances in Materials Science, Vol. 17, iss. 52, pp. 1-16, 2017, doi: 10.1515/adms-2017-0007

[9] N.P. Abbade, S.J. Crnkovic, *Sand–water slurry erosion of API 5L X65 pipe steel as quenched from intercritical temperature,* Tribology International, vol. 33, iss. 12, pp. 811–816, 2000, doi: 10.1016/S0301-679X(00)00126-2

[10] G. Krauss, *Steels: Heat treatments and processing principles.* 4th ed Materials Park, USA: ASM International, 1995.

[11] K.E. Thelning, *Steel and its treatment,* 2nd Ed UK: Butterworths, 1984.

[12] W.L. Roberts, *Hot rolling of steel*. In: Manufacturing Engineering and Materials Processing, vol. 10. New York: Marcel Dekker, 1983.

[13] I. Karaman, H. Sehitoglu, Y.I. Chumlyakov, H.J.Maier, *The deformation of low-stacking-fault-energy austenitic steels*. *JOM*, vol. 54, iss. 7, pp. 31-37,2002, doi : 10.1007/BF02700983

[14] C.T. Kwok, H.C. Man, F.T. Cheng, *Cavitation erosion of duplex and super duplex stainless steels,* Scripta Materialia, vol. 39, iss. 9, pp. 1229-1236, 1998, doi: 10.1016/S1359-6462(98)00308-X

[15] R. Schramm, R. Reed, *Stacking fault energies of seven commercial austenitic stainless steels*, Metallurgical Transactions *A*, vol. 6, iss. 7, pp. 1345-1351, 1975, doi: 10.1007/BF02641927

[16] A. Karimi, *Cavitation erosion of a duplex stainless steel*, Materials Science and Engineering, vol. 86, pp. 191-203, 1987, doi: 10.1016/00255416(87)904526

[17] X. Xu, S. van der Zwaag, W. Xu, *The effect of ferrite–martensite morphology on the scratch and abrasive wear behaviour of a dual phase construction stee*l, Wear, vol. 348-349, pp. 148-157, 2016, doi: 10.1016/j.wear.2015.12.005

[18] Xiaojun Xu, Sybrand van der Zwaag, Wei Xu, *The effect of martensite volume fraction on the scratch and abrasion resistance of a ferrite–martensite dual phase steel*, Wear, vol. 348-349, pp. 80-88, 2016, doi: 10.1016/j.wear.2015.11.017

[19] S. Aribo, R. Barker, X. Hu, A. Neville, *Erosion–corrosion behaviour of lean duplex stainless steels in 3.5%NaCl solution,* Wear, vol. 302, iss. 1-2, pp. 1602-1608, 2013, doi: 10.1016/j.wear.2012.12.007

[20] F. Mohammadi, J. Luo, *Effect of cold work on erosion–corrosion of 304 stainless steel,* Corrosion Science, vol. 53, iss. 2, pp. 549-556, 2011, doi: 10.1016/j.corsci.2010.09.059

[21] A.V. Levy, N. Jee, P. Yau, *Erosion of steels in coal-solvent slurries,* Wear, vol. 117, iss. 2, pp. 115–127, 1987, doi: 10.1016/0043-1648(87)90250-X

[22] A. Levy, G. Hickey, *Liquid–solid particle slurry erosion of steels*, Wear, vol. 117, iss. 2, pp. 129–46, 1987, doi: 10.1016/0043-1648(87)90251-1

[23] M.C. Roco, P. Nair, G.R. Addie, *Test approach for dense slurry erosion*. in: J.E. Miller, Jr. F.E. Schimidt, editors. Slurry Erosion: Uses, Applications, and Test Methods, ASTM Spec. Tech. Publ. 946, pp. 185-210, 1987.

[24] J.B. Zu, I.M. Hutchings, G.T. Burstei, *Design of a slurry erosion test rig*, Wear vol. 140, iss. 2, pp. 331–334, 1990, doi: 10.1016/0043-1648(90)90093-P

[25] A.A. Gorni, *Steel forming and heat-treating hand book*, vol. 2, Saova Center, Brazil, p. 4, 2004.

[26] S. Aribo, A. Fakorede, O. Ige, P. Olubambi, *Erosion-corrosion behaviour of aluminium alloy 6063 hybrid composite*, Wear, vol. 376-377, pp. 608-614, 2017, doi: 10.1016/j.wear.2017.01.034

[27] S.G. Sapate, A.D. Chopde, P.M. Nimbalkar, D.K. Chandrakar, *Effect of microstructure on slurry abrasion response of EN-31 steel*, Materials and Design, vol. 29, iss. 3, pp. 613-621, 2008, doi: 10.1016/j.matdes.2007.02.014

[28] S. Tekeli, A. Gural, *Dry sliding behaviour of heat treated iron based powder metallurgy steels with 0.3 Graphite + 2% Ni additions*, Materials and Design, vol. 28, iss. 6, pp. 1923-1927, 2007, doi: 10.1016/j.matdes.2006.05.009